

# Synthesis of poly(dimethylsiloxane) and poly(butadiene) composite particles and the properties of their grafted polymer particles

M. Okaniwa\*

*Tsukuba Research Laboratory, JSR Corporation, 25 Miyukigaoka, Tsukuba, Ibaraki 305-0841, Japan*

Received 18 February 1999; accepted 1 March 1999

## Abstract

Micro separated composite polymer particles comprising of poly(dimethylsiloxane) (PDMS) and poly(butadiene) (PB) were prepared by an emulsifier-free seeded emulsion polymerization of butadiene with a radical initiator in the presence of a PDMS latex. The following three factors controlled the morphology of the particles: (i) cross-linking degree of PDMS; (ii) cross-linking degree of PB; and (iii) source of polymerization initiator. By decreasing the cross-linking degree of PDMS or PB, we obtain segregated PB from PDMS. An initiation system consisting of *tert*-butyl peroxyaurate and ferrous sulfate gave the hemispherical morphology in contrast to the core shell for potassium persulfate. Styrene and acrylonitrile were able to graft onto the PB phase of the particles with high efficiency. The corrections between the morphology of the composite polymer particles and the practical properties of poly(styrene-*co*-acrylonitrile)-modified graft polymers were also discussed. © 1999 Elsevier Science Ltd. All rights reserved.

*Keywords:* Morphology; Composite polymer particles; Poly(dimethylsiloxane)

## 1. Introduction

High impact resistance polymers such as ABS [poly(styrene-*co*-acrylonitrile)-*graft*-poly(butadiene)] and high impact poly(styrene) (HIPS) [poly(styrene)-*graft*-poly(butadiene)] are based on the two-phase polymer system, comprising a continuous glassy phase containing finely dispersed poly(butadiene) (PB) particles [1–7]. To stabilize these two domains, grafting the monomer onto the PB was employed [8–11]. The PB toughened resins, however, show poor weather resistance caused by the oxidation of PB after periods of outdoor exposure. To overcome this problem, saturated polymers such as poly(ethylene-*co*-propylene) [12], acrylate rubber [13], and poly(dimethylsiloxane) (PDMS) [14], were employed as dispersed rubbery domains. The domains generally consist of a single polymer, however, if micro separated composite polymer particles (CPS) consisting of two polymers can be used as domains, this material will show interesting properties derived from the two polymers. The author recently reported that PDMS and poly(tetrafluoroethylene) surface are inert against radical grafting, however, the surface was able to be modified by PB coating. Then, poly(styrene-*co*-acrylonitrile) (SAN) was successfully grafted onto the PB

shell with high efficiency [15–18]. In this article, the SAN grafted CPS consisting of PDMS and PB were prepared; the relationship between the morphologies of CPS and the practical properties of the graft polymer will be discussed.

## 2. Experimental

### 2.1. Materials

Octamethylcyclotetrasiloxane (Toshiba Silicone), methyltriethoxysilane (Toshiba Silicone), *n*-dodecylbenzenesulfonic acid (Kao), styrene (Mitsubishi Chemical), acrylonitrile (Mitsubishi Chemical), potassium laurate (Nippon Oil and Fats) and sodium carbonate (Asahi Chemical) were used as-received. Potassium persulfate, iron(II) sulfate heptahydrate, dextrose sodium pyrophosphate, calcium chloride, 2-butanone, *tert*-dodecanetriol and toluene were purchased from Wako Pure Chemical Industry and used without further purification. *Tert*-butyl peroxyaurate and diisopropylbenzene hydroperoxide (commercial grade from Nippon Oil and Fats) were used as-received. Butadiene and SAN resin (no. 290NC, AN content 25%) was of commercial grade from JSR Co. Ltd.

### 2.2. Weight percent of cross-linked polymer molecules

The weight percent of cross-linked polymer molecules

\* Tel.: +81-298-56-1109; fax: +81-298-56-1504.

*E-mail address:* motoki\_okaniwa@jsr.co.jp (M. Okaniwa)

Table 1  
The conditions used in the preparation of the PDMS latex

PDMS no.	1	2
Octamethylcyclotetrasiloxane (g)	300	288
Methyltriethoxysiloxane (g)	–	12
Deionized water (g)	450	450
93% n-dodecylbenzenesulfonic acid (g)	6.45	6.45
Insoluble polymer part ( $f_{\text{network}}$ ) in toluene (%)	0	57
$M_w$	612 000	–
$M_n$	183 000	–

was determined by the modified Sakurai's method [19]. The mixture consisting of the dried polymer ( $w_0$ :0.15 g) and toluene (20 ml) was shaken for 24 h at room temperature. Thus, the uncross-linked polymer molecules dissolved and diffused out of the bulk polymer. The mixture was separated into a soluble fraction for toluene and insoluble fraction with filter paper. The 5 ml soluble fraction for toluene was poured into a tarred aluminum pan and dried, first for 10 min at 120°C, and then for 24 h at 80°C in vacuo. The weight percent of cross-linked polymer molecules,  $f_{\text{network}}$ , was determined by the following equation:

$$f_{\text{network}} = (100 - w_f/w_0 \times 4) \times 100,$$

where  $w_f$  is the weight of the soluble fraction for toluene. Replicate determination was performed for each latex recipe, and the weight percents of cross-linked polymer molecules averaged.

### 2.3. Preparation of poly(dimethylsiloxane) latex

Linear (1) and cross-linked PDMS latex (2) were prepared by cationic polymerization of siloxane monomer initiated by *n*-dodecylbenzenesulfonic acid using the conditions previously described [20]. Table 1 gives the polymerization recipes for the PDMS latex. Polymerization was quenched by neutralization through the addition of sodium

Table 2  
The conditions used in the preparation of composite particles of PDMS and PB

Composite particle of PDMS and PB	A	B	C	D	E	F
PDMS no. <sup>a</sup>	1	1	2	2	2	2
35% PDMS latex (g)	143	143	143	143	143	143
Butadiene (g)	50	50	50	50	50	50
3% potassium persulfate (g)	–	33	33	33	33	33
Tert-butylperoxylaurate (g)	0.47	–	–	–	–	–
The reductant solution						
Ferrous sulfate heptahydrate (mg)	4	–	–	–	–	–
Dextrose (g)	0.25	–	–	–	–	–
Sodium pyrophosphate (g)	0.2	–	–	–	–	–
Deionized water (g)	8	–	–	–	–	–
Tert-dodecanetriol (g)	–	–	–	0.5	1	1.5
Run time (h)	12	24	24	24	24	24

<sup>a</sup> See Table 1.

carbonate (pH = 7.0). The molecular weight of 1 was measured by gel permeation chromatograms in toluene on a Waters 510 pump chromatograph with Shodex K-80M and K-802 columns equipped with an RI detector (Waters 410) on the basis of polystyrene calibration. The weight-average molecular weight of the polymer was 612 000; the number-average molecular weight was 183 000. The  $f_{\text{network}}$  of 1 and 2 were 0 and 57%, respectively.

### 2.4. Preparation of CPS consisting of PDMS and PB

CPS consisting of PDMS and PB were prepared by emulsifier-free seeded emulsion polymerization of butadiene with a radical initiator in the presence of PDMS seed particles. Table 2 shows the polymerization recipes for the composite particles. The polymerization was carried out in a 300 ml high-pressure bottle. Thirty-five percent uncross-linked PDMS latex 2 (143 g), *tert*-butyl perlaurate (0.471 g), and the reductant solution [ferrous sulfate heptahydrate (4.0 mg), dextrose (0.25 g), sodium pyrophosphate (0.20 g) and deionized water (8.0 g) were added to the reactor, and the bottle sealed and evacuated. Butadiene (50 g) was charged to the reactor, and the system was aged at 65°C for 24 h (yield = 98%). The conversion of butadiene was measured by the gravimetry of the non-volatile compounds. The obtained latex of composite particles was kept for 4 h at 70°C under nitrogen bubbling to evaporate any unreacted butadiene. The  $f_{\text{network}}$  was 54%. The polymer soluble fraction in toluene consisted of not cross-linked PDMS and not cross-linked PB.

### 2.5. Preparation of the graft copolymer

The graft polymer latexes were prepared using the conditions described previously [15]. The raw dry products (40 wt.%) blended with SAN (60 wt.%) were molded with a twin screw extruder at 230°C. The test samples were obtained by injection molding of the blends at 230°C.

### 2.6. Graft ratio, grafting efficiency and intrinsic viscosity of non-graft copolymer

The graft ratio, grafting efficiency and intrinsic viscosity of non-graft copolymer were determined as previously described [15].

### 2.7. Transmission electron micrograph observation

The latex of CPS was exposed to osmic acid vapor at room temperature for 30 min for definition, and observed with a transmission electron micrograph (TEM). The ultrathin cross-section of the molded sample was also stained by osmic acid and observed with the TEM.

### 2.8. Izod impact strength

The Izod impact strength was measured according to ASTM D-256 (Izod with notched specimens).

Table 3  
Effect of cross-link density of PDMS or PB and initiation mode on the properties of the composite particles

Sample <sup>a</sup>	No. of seed PDMS <sup>b</sup>	PDMS $f_{\text{network}}$	Initiator/reductant	Addition of tert-dodecanethiol (phr)	Conversion of butadiene (%)	Composite particle		Diameter ( $\mu\text{m}$ ) <sup>c</sup>		Morphology		Figure
						$f_{\text{network}}$	Composition	Inner	Outer	Architecture	PB new particles	
A	1	0	TBL/ferrous sulfate	none	98	54	54/46	0.15	–	Hemispherical	No	Fig. 1(a)
B	1	0	KPS	none	95	66	53/47	0.15	0.19	Core-shell	Yes	Fig. 1(b)
C	2	57	KPS	none	87	88	57/43	0.17	0.25	Core-shell	No	Fig. 1(c)
D	2	57	KPS	0.5	89	65	56/44	0.17	–	Hemispherical	No	–
E	2	57	KPS	1	88	52	56/44	0.17	–	Hemispherical	No	–
F	2	57	KPS	1.5	89	45	56/44	0.17	–	Hemispherical	No	Fig. 1(d)

<sup>a</sup> See Table 2.

<sup>b</sup> See Table 1.

<sup>c</sup> Determined by TEM of graft polymer particles because the composite particle with not cross-linked PDMS (I) melted by the exposure to electron beam of TEM.

### 2.9. Surface gloss

Surface gloss was measured according to ASTM D-523 (reflection angle, 45°).

### 2.10. Melt flow rate

Melt flow rate was measured according to JIS K7210 (test temperature, 220°C).

### 2.11. Percent elongation

Percent elongation was measured according to ASTM D-635-56T (test speed, 50 mm/min).

### 2.12. Tensile strength

Tensile strength was measured according to ASTM D-638-52T (test speed, 50 mm/min).

### 2.13. Sliding wear resistance

Sliding wear resistance was measured using the conditions described previously [16].

## 3. Results and discussion

During the synthesis of micro separated CPS, many of the polymerization parameters and conditions are known to affect the CPS morphology, for example, the water solubility of the monomer, viscosity of the polymerization loci, initiation mode, and the degree of grafting of the second stage polymer onto the core particle [21–24]. Depending on the polymerization parameters and conditions, polymer particles with heterogeneous structures are formed. The heterogeneous structure involves a core-shell, inverted core-shell, hemispheres, double-ball, sandwich, raspberry-like and void particles.

At the beginning of the reaction, butadiene (BD) monomers are absorbed in the PDMS particles because PDMS possess a high swelling ability against monomer [25], and BD is hydrophobic. The initiation locus of BD is different from the source of initiator's hydrophobicity. In the presence of potassium persulfate (KPS) as a water-soluble initiator, the main locus of radical formation is the aqueous phase [26,27]. PB oligomer, which consists of one to three monomeric units, exists in aqueous phase, then the polymerization locus migrates from the water phase to the interior of the monomer-swollen polymer particle with the increasing hydrophobicity of PB [28,29]. By contrast, in the presence of oil soluble-initiator, the main locus of radical formation can be considered as the interior of the PDMS particles from the beginning to the end of polymerization. As BD polymerization proceeds, PB polymers are segregated from the PDMS particles. The most stable segregated morphology is determined by the balance of their surface tension, i.e. water–PDMS, PDMS–PB, water–PB. Various kinds of

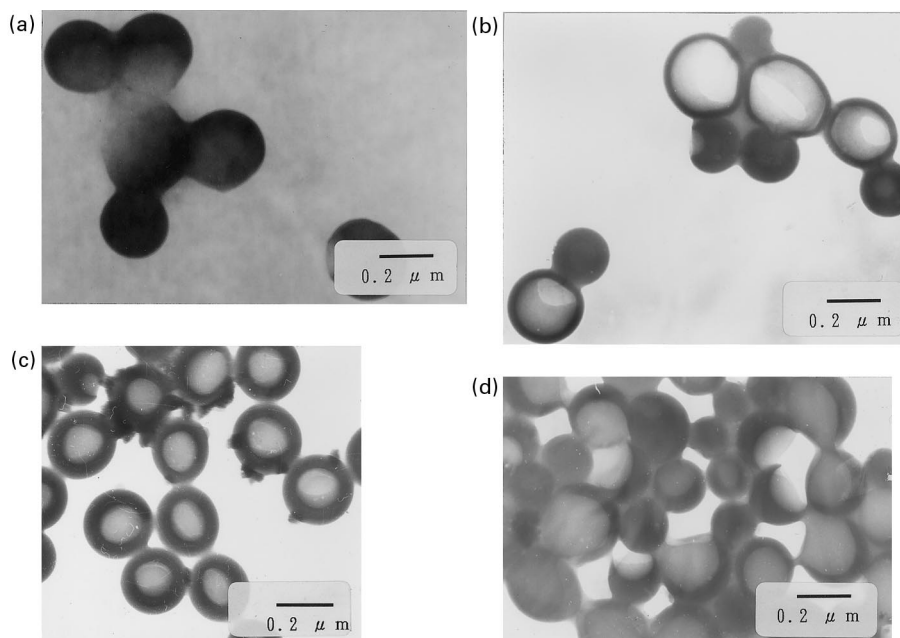


Fig. 1. TEM of composite particles of PDMS and PB: (a) sample A; (b) sample B; (c) sample C; and (d) sample F (Table 2).

morphologies, however, could be obtained in the case of the following situations: high viscosity of the reaction locus; generation of a chemical bond between PDMS and PB with a grafting initiator; and change of polymer mobility caused by cross-linking reaction. The morphologies of the CPS will control the practical properties of the CPS toughened resins. It is also interesting to examine the relationship between the morphologies of the CPS and the practical properties of the CPS toughened resin. Thus, in Section 3.1, I focused on controlling the morphology of the CPS. The morphologies can be controlled by any of the following three factors: (1) the cross-linking degree of the PDMS, (2) the cross-linking degree of the PB, and (3) the source of the polymerization initiator. In Section 3.2, the relationship between the morphologies of CPS and the practical properties of SAN modified resin will be discussed.

### 3.1. Controlling morphology of CPS consisting of PDMS and PB

CPS were prepared by an emulsifier-free seeded emulsion polymerization of BD with a radical initiator in the presence of PDMS latex. The reaction conditions and results are summarized in Table 3. Fig. 1 shows the TEM pictures of CPS stained by osmic acid. The PDMS and PB are light and dark region of the particles, respectively.

#### 3.1.1. Effect of cross-linking degree of PDMS

The cross-linking degree of PDMS was found to be controlled by the addition of methyltriethoxysilane as a cross-linking agent as described in Table 1. CPS were prepared under the same conditions (initiator: KPS, without a *tert*-dodecanetriol), except for the source of PDMS (linear

PDMS **1** or cross-linked PDMS **2**). The results are shown in Table 3 (for samples B and C) and in Fig. 1(b) and (c). PB secondary particles were generated with linear PDMS **1** as seed latex (Fig. 1(b)). This is because the mobility of PB chains in PDMS particles could increase; then, PB gets segregated from PDMS to form PB secondary particles. However, the PB secondary particles were able to be suppressed with cross-linking PDMS **2** (Fig. 1(c)). This is because the mobility of the PB in the cross-linking PDMS would decrease and therefore, the segregation from PDMS particles was suppressed.

#### 3.1.2. Effect of cross-linking degree of PB

The effect of the cross-linking degree of PB on the

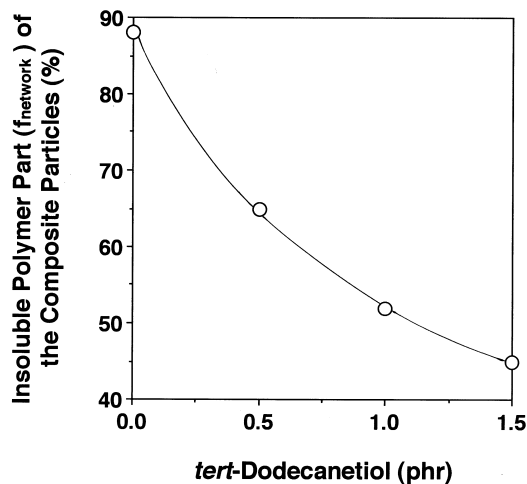


Fig. 2. Effect of *tert*-dodecanetriol content on the insoluble polymer part of the composite polymer particles comprised PDMS and PB.

Table 4  
Free energy change for the formation of composite particles consisting of PDMS and PB

Sample <sup>a</sup>	Morphology	$r_{\text{PDMS}}^b$ ( $\times 10^{-9}$ m)	$r_{\text{PB}}^c$ ( $\times 10^{-9}$ m)	$h_{\text{PDMS}}^d$ ( $\times 10^{-9}$ m)	$h_{\text{PB}}^e$ ( $\times 10^{-9}$ m)	Equation	$\Delta G$ ( $\times 10^{-17}$ J)	$\Delta G_{\text{hemispherical}} - \Delta G_{\text{core-shell}}$ ( $\times 10^{-17}$ J)
C	Core-shell	8.5	12.5	–	–	(1)	2.08 <sup>a</sup>	0
F	Hemispherical	8.5	11.7	13.3	11.7	(2)	– 2.23 <sup>b</sup>	– 4.31

<sup>a</sup> See Table 3.

<sup>b</sup>  $r_{\text{PDMS}}$ : radius of the spherical portion of original PDMS phase.

<sup>c</sup>  $r_{\text{PB}}$ : radius of the spherical portion of secondary PB phase.

<sup>d</sup>  $h_{\text{PDMS}}$ : apparent penetration distance of the original PDMS phase into the secondary PB phase.

<sup>e</sup>  $h_{\text{PB}}$ : apparent penetration distance of the secondary PB phase into the original PDMS phase.

$$\Delta G_{\text{core-shell}} = \gamma_{\text{PDMS-PB}} 4\pi r_{\text{Si}}^2 + \gamma_{\text{PB-Water}} 4\pi r_{\text{PB}}^2 - \gamma_{\text{PDMS-Water}} 4\pi r_{\text{Si}}^2 \quad (1)$$

$$\Delta G_{\text{Hemispherical}} = \gamma_{\text{PDMS-Water}} [2\pi(2r_{\text{PDMS}}^2 - 2r_{\text{PDMS}}h_{\text{PDMS}})] + \gamma_{\text{PDMS-PB}} [2\pi(2r_{\text{PB}}^2 - 2r_{\text{PB}}h_{\text{PB}})] + \gamma_{\text{PB-Water}} (2\pi r_{\text{PDMS}}h_{\text{PDMS}} - \pi h_{\text{PDMS}}^2) - \gamma_{\text{PB-Water}} 4\pi R_{\text{PDMS}}^2 \quad (2)$$

where  $R_{\text{PDMS}} = [\gamma_{\text{PDMS}}^2 - (h_{\text{PDMS}}^2/4)(3r_{\text{PDMS}} - h_{\text{PDMS}})]^{1/3}$ ,  $\gamma_{\text{PDMS-PB}}$  ( $4.66 \times 10^{-3}$  J/m<sup>2</sup>)<sup>32</sup> is the interfacial surface tension between PDMS and PB,  $\gamma_{\text{PB-Water}}$  ( $3.04 \times 10^{-3}$  J/m<sup>2</sup>)<sup>15</sup> is the interfacefree energy of PDMS against water, and  $\gamma_{\text{PDMS-Water}}$  ( $4.75 \times 10^{-3}$  J/m<sup>2</sup>)<sup>15</sup> is the interfacefree energy of PDMS against water.

morphologies of CPS was also investigated. Cross-linking density of PB could be controlled by the addition of *tert*-dodecanetriol as chain transfer agents [30]. Polymerization of BD were performed in a similar manner (initiator: KPS, PDMS: cross-linked PDMS **2**), with the exception of the feed amounts of *tert*-dodecanetriol. The results were also shown in samples C and F (Table 3), and Fig. 2. Fig. 2 shows the relationship between the feed amounts of *tert*-dodecanetriol and the cross-linking density of CPS. The increase of *tert*-dodecanetriol feed amounts results in a decrease in PBs cross-linking density of CPS. It was also found that decreasing cross-linking density of PB alters the morphology from core-shell (Fig. 1(c)) to hemispherical (Fig. 1(d)). This is because the mobility of PB increases with the decrease of PB's cross-link density, therefore, the segregation of PB from PDMS could proceed. The thermodynamic analysis of CPS reported by Sundberg is listed in Table 4 [31,32]. The calculations indicate that the hemispherical structure represents a thermodynamically favored structure compared to the core-shell structure, i.e. the cross-linking of PB prevents the conversion of a stable morphology and gives rise to starvation conditions. Jonsson et al. studied the morphology of a two-phase poly(styrene) (PS)/poly(methyl methacrylate) (PMMA) prepared under different polymerization conditions [33]. The two-phase latex particles were prepared by polymerizing, at 60°C, MMA in the presence of monodisperse PS seed particles. Intermittent swelling of the two-phase particles, by addition and subsequent removal of methylene chloride from the latex, produced composite particles containing one PS domain, partly engulfing a seemingly spherical PMMA domain (double-ball structure). It was concluded that this double-ball structure represents a thermodynamically favored, metastable situation for PS/PMMA composite particles in water.

### 3.1.3. Effect of the source of polymerization initiator

The effect of the source of polymerization initiator on the

morphologies of CPS was also examined. An initiation system consisting of *tert*-butyl perlaurate (TBL) coupled with ferrous sulfate is hydrophobic, and possesses efficient grafting ability, in contrast to the KPS initiator. CPS were synthesized under the same condition except for a source of polymerization initiator (PDMS; linear PDMS **1**, without *tert*-dodecanetriol). The result using the TBL initiator is shown for sample A in Table 3 and Fig. 1(a). In the presence of TBL initiator, no PB secondary particle can be generated even though the seed particles were not cross-linked. The morphology of CPS was found to be a hemispherical structure (Fig. 1(a)). The formation of this hemispherical structure was considered as follows: (i) because of the high grafting ability of TBL initiator [16], it can be considered that grafting of BD onto the PB shell as well as the propagation reaction of PB progresses. The grafting could proceed exclusively on the PB phase formed at the PDMS particles because the grafting reactivity of

Table 5

Properties of the graft polymer particles (composition: graft polymer/SAN = 40/60 (wt.%) and rubber content was 16 wt.%)

Composite particles as seed <sup>a</sup>	A	B	C
TEM of the inner of the moulded sample	Fig. 3(a)	Fig. 3(b)	Fig. 3(c)
SEM of the surface of the moulded sample	Fig. 4(a)	Fig. 4(b)	Fig. 4(c)
Grafting efficiency (%)	50	79	78
Graft ratio (%)	75	118	117
$[\eta]_{\text{MEK}}^{30^\circ\text{C}}$	0.46	0.47	0.60
Composition of PDMS/PB	8.5/7.5	9.0/7.0	8.6/7.4
Izod impact strength (J/m)	157	73	98
Surface gloss	82	47	86
Melt flow rate (g/10 min)	10	30	10
Percent elongation	34	6	58
Tensile strength (MPa)	49	36	47
Coefficient of friction	0.17	0.31	0.14
Wear (mg)	0.84	3.23	1.13

<sup>a</sup> See Table 3.

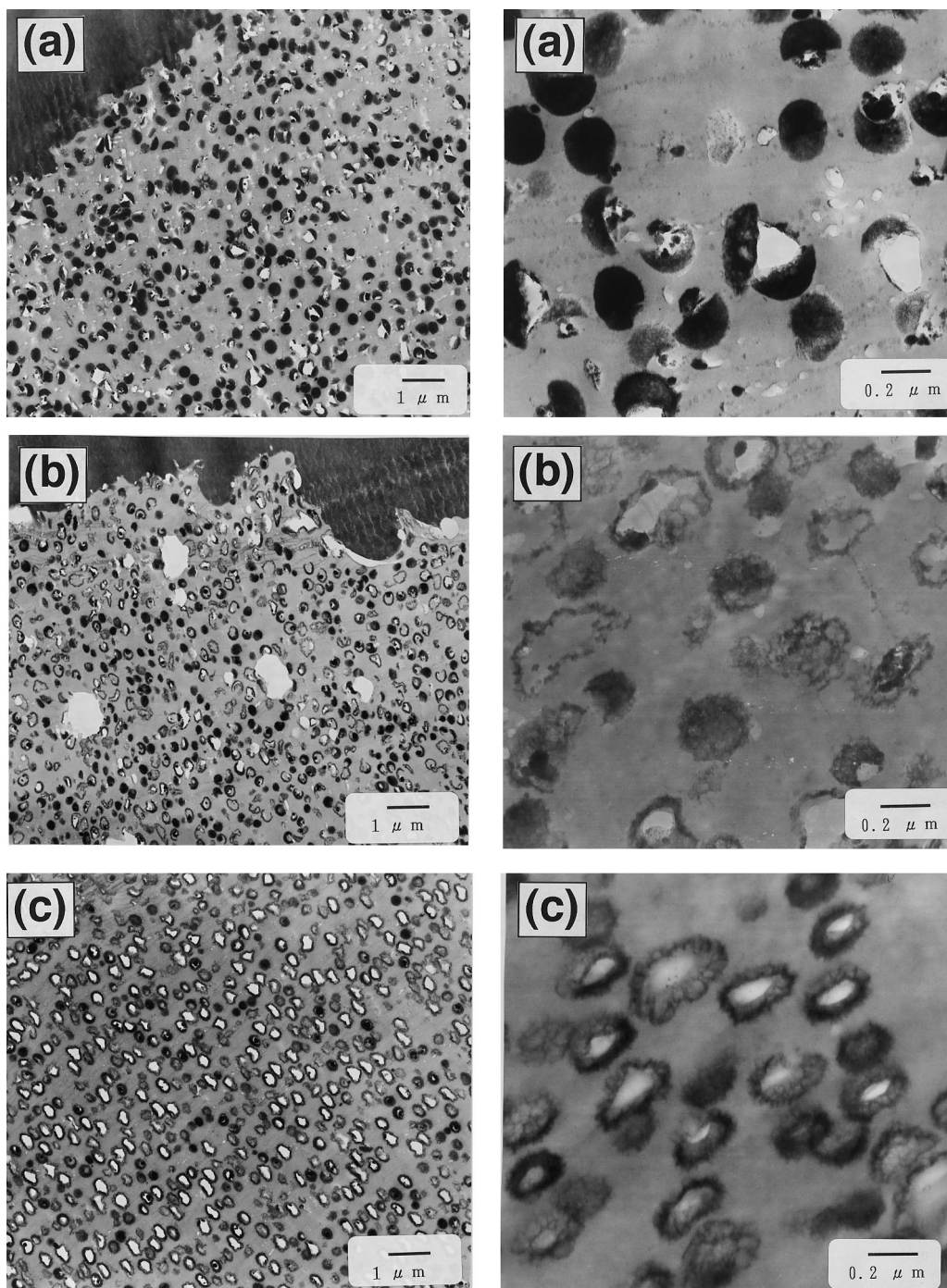


Fig. 3. TEM of the blends of grafted polymer and SAN: (a) sample A; (b) sample B; and (c) sample C (Table 5).

PB is much higher than that of PDMS [15]. (ii) The cross-link density of CPS obtained with TBL initiator was smaller than that obtained with KPS. Increasing the mobility of PB leads to the formation of a thermodynamically stable hemispherical structure. Cook et al. reported that during the synthesis of CPS consisting of PS and poly(butyl acrylate) (PBA), the limited water solubility of AIBN decreases the formation of PS secondary particles [34].

### 3.2. Relationship between the morphology of CPS and practical properties of CPS toughened SAN

Table 5 shows the practical properties of CPS toughened resin, i.e. izod impact strength, tensile strength, melt flow rate, surface gloss, and lubricity. The molded sample of the TEM and the SEM pictures were shown in Figs. 3 and 4, respectively. Fig. 5 shows the morphologies of CPS, graft copolymers and molded samples. Morphology of the

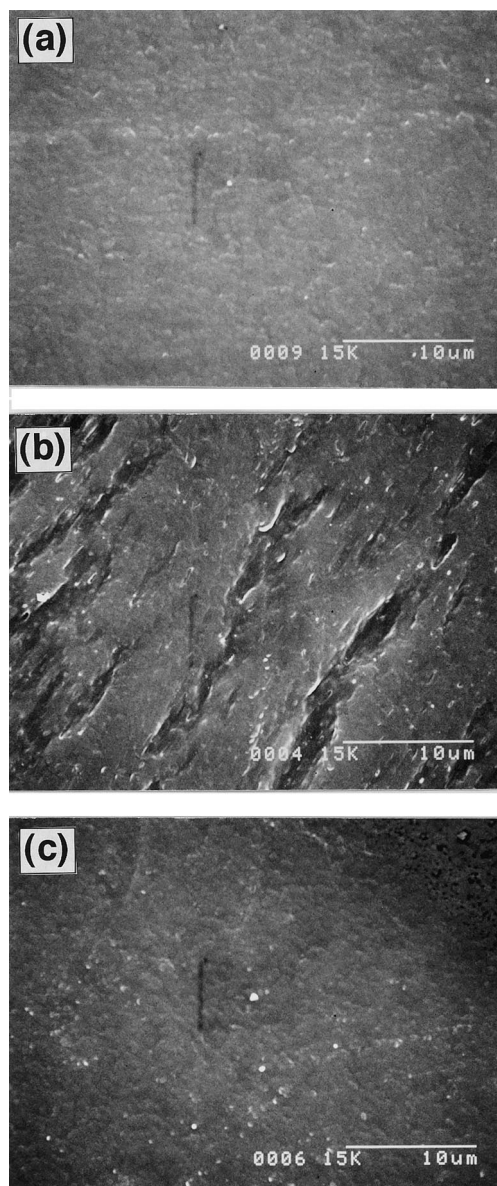


Fig. 4. SEM of the blends of grafted polymer and SAN: (a) sample A; (b) sample B; and (c) sample C (Table 5).

molded sample is almost similar to the morphology of the original CPS. However, the aggregated PDMS particles were observed in sample B (Fig. 3(b)). The aggregated PDMS particles were produced by the coalescence of uncovered PDMS, which could not be observed in the TEM picture (Fig. 1(b)), as PDMS could not be stained by osmic acid. The PDMS uncovered by PB will remain after the grafting of SAN because no grafting onto PDMS proceeded in the presence of diisopropylbenzene hydroperoxide as a common graft initiator [16].

### 3.2.1. Relationship between CPS morphology and grafting efficiency

As summarized in Table 5, grafting efficiency significantly depended on the CPS used. The grafting efficiency

of the hemispherical structure (sample A) is much smaller than that of the core-shell structure even though the PB amount in each CPS was constant. This is because the PB surface area of the hemispherical CPS is smaller than that of the core-shell.

### 3.2.2. Relationship between CPS morphology and practical properties of CPS toughened resin

**Surface gloss.** The surface gloss of a molded sample is related to the surface unevenness of samples. Low surface gloss of sample B was caused by the existence of large PDMS particles, which are larger than the visible spectrum (TEM picture, Fig. 3(b); SEM picture, Fig. 4(b)). However, high surface gloss for samples A and C (SEM picture, Fig. 4(a) and (c)) can be achieved by homogeneous submicron-size dispersion of CPS (as seen in the TEM pictures, Fig. 3(a) and (c)).

**Izod impact strength and tensile strength.** Impact and tensile strengths of sample B was fairly lower than that of the other samples. The reason for this is considered to be that the KPS initiator cannot produce PB graft chains surrounding the PDMS particles. Due to the absence of the graft chain, no grafting of SAN onto the PDMS can proceed, eventually, the PDMS gets segregated from SAN to form PDMS large domain. The aggregated PDMS particles act as stress concentration points at the impact test. Good impact resistance of sample A is due to the existence of PB graft chains, which can be produced by TBL initiator [16].

**Lubricity.** The coefficient of friction and wear amounts show lubricity of materials. PDMS is known to be one of the good lubricity materials, therefore, lubricity of a sample is related to the PDMS concentration at the surface of test piece. Lubricity of samples A and B are better than that of sample C because PDMS in sample C was covered by a PB shell, and SAN was grafted efficiently. To improve the lubricity, blending of untreated PDMS into resins was proposed. This method, however, induces drastic decrease in both the impact and tensile strengths, as shown for sample B. Apparently, in sample B a tendency to demix and exude free PDMS polymer at the surface was observed. Furthermore, PDMS coated at the surface of resins will be consumed after long periods of friction and wear test. Therefore, to maintain good lubricity, a troublesome process, i.e. coating of PDMS constantly onto a surface is required. These problems can be solved by controlling the CPS morphology, as shown in sample A (Fig. 1(a)).

It was found that the properties of CPS toughened resin closely related to the CPS morphology. By controlling the morphology the CPS toughened resin with the TBL initiator demonstrated successful application as impact and surface lubricity modifier of SAN. I believe that micro separated composite polymer particles will offer interesting possibility as novel rubbery dispersion particles of toughened resins.

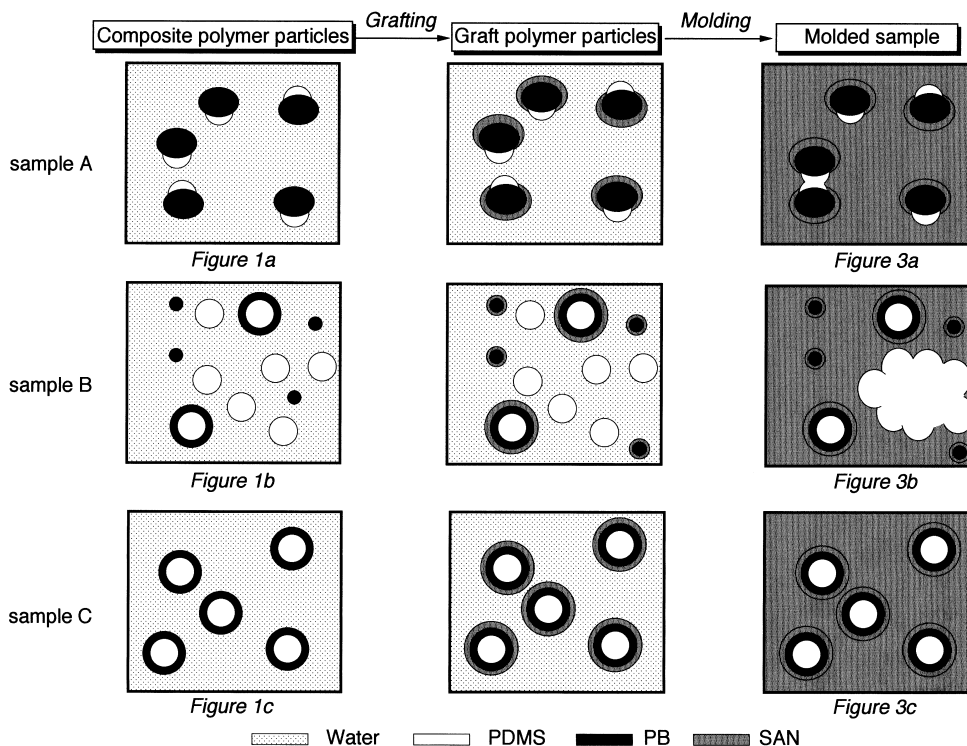


Fig. 5. Morphologies of the composite polymer particles; graft polymer particles; and molded sample.

## Acknowledgements

The author thanks Mr. K. Hirose for measurements of the TEM and SEM observations. Thanks are also due to Mr. A. Shiota and Dr. C. Ballard for their comments and suggestions during the preparation of this manuscript.

## References

- [1] Narisawa I, Kuriyama T, Ojima K. *Macromol Chem, Macromol Symp* 1991;41:87.
- [2] Dagli G, Argon AS, Cohen RE. *Polymer* 1995;36:2173.
- [3] Souheng W. *Polym Engng Sci* 1990;30:753.
- [4] Cigna G, Maestrini C, Castellani L, Lomellini P. *J Appl Polym Sci* 1992;44:505.
- [5] Hobbs SY. *Polym Engng Sci* 1986;26:74.
- [6] Goto H, Kuratani K, Ogura K. *Kobunshi Ronbunshu* 1994;51(9):586 in Japanese.
- [7] Goto H, Kuratani K, Kito H, Shimono T, Ogura K. *Kobunshi Ronbunshu* 1994;51(11):752 in Japanese.
- [8] Huang NJ, Sundberg DC. *J Polym Sci, Polym Chem Ed* 1995; 33:2533.
- [9] Huang NJ, Sundberg DC. *J Polym Sci, Polym Chem Ed* 1995; 33:2551.
- [10] Huang NJ, Sundberg DC. *J Polym Sci, Polym Chem Ed* 1995; 33:2571.
- [11] Huang NJ, Sundberg DC. *J Polym Sci, Polym Chem Ed* 1995; 33:2587.
- [12] Sevrini F, Pegoraro M, Landro LD. *Angew Macromol Chem* 1991;190:177.
- [13] Min TI, Klein A, El-Aasser MS, Vanderhoff JW. *J Polym Sci, Polym Chem Ed* 1983;21:2845.
- [14] Saam JC, Mattler CM, Falender JR, Dill TJ. *J Appl Polym Sci* 1979;24:187.
- [15] Okaniwa M, Kawahashi N. *Colloid Polym Sci* 1997;275:315.
- [16] Okaniwa M, Ohata Y. *J Polym Sci, Polym Chem Ed* 1997;35:2607.
- [17] Okaniwa M. *J Appl Polym Sci* 1998;68:185.
- [18] Okaniwa M. Recent research development in polymer science. *Trans-world research network*, vol. 3, 1998
- [19] Sakurai S, Iwane K, Nomura S. *Macromolecules* 1993;26:5479.
- [20] Weyenberg DR, Findlay DE, Cekada J, Bey AE. *J Polym Sci, Polym Symp Ed* 1969;27:27.
- [21] Chen YC, Dimonie V, El-Aasser MS. *J Appl Polym Sci* 1991;42:1049.
- [22] Sundberg EJ, Sundberg DC. *J Appl Polym Sci* 1993;47:1277.
- [23] Lee S, Rudin A. *J Polym Sci, Polym Chem Ed* 1992;30:865.
- [24] Durant YG, Sundberg DC. *Macromolecules* 1996;29:8466.
- [25] Favre E. *Eur Polym J* 1996;32(10):1183.
- [26] Daniels ES, Dimonie VL, El-Aasser MS, Vanderhoff JW. *J Appl Polym Sci* 1990;41:2463.
- [27] Maxwell IA, Morrison BR, Napper DH, Gilbert RG. *Macromolecules* 1991;24:1629.
- [28] Kshirsagar RS, Poehlein GW. *J Appl Polym Sci* 1994;54:909.
- [29] Ammerdorffer JL, Lemmens AAG, German AL, Everaerts FM. *Polym Commun* 1990;31:61.
- [30] Weerts PA, Loos JLM, German AL. *Macromol Chem* 1991;192:2009.
- [31] Sundberg DC, Casassa AP, Pantazopoulos J, Muscato MR. *J Appl Polym Sci* 1990;41:1425.
- [32] Fleischer CA, Koberstein JT, Krukonis V, Wetmore PA. *Macromolecules* 1993;26:4172.
- [33] Jonsson JEL, Hassander H, Jansson LH, Tornell B. *Macromolecules* 1991;24:126.
- [34] Cook DG, Rudin A, Plumtree A. *J Appl Polym Sci* 1992;46:1387.